Experimental and Numerical Characterization of Thermal Bridges in Prefabricated Building Walls

Laurent Zalewski[a*], Stéphane Lassue[a], Daniel Rousse[b], Kamel Boukhalfa[a]

[a]*Laboratoire d'Artois Mécanique Thermique et Instrumentation, Université d'Artois, Béthune, France*

[b]*Department of mechanical engineering, École de technologie supérieure, Montréal, H3C 1K3, Canada*

Abstract

This work is a contribution to the characterization of the thermal efficiency of complex walls of buildings with respect to the ever increasing requirements in thermal insulation. The work specifically concerns the quantitative evaluation of heat losses by thermal bridges. The support of the study is the envelope of industrial light construction walls containing a metal framework, an insulating material inserted in between metal trusses, water and vapor barriers, and the internal and external facings. This article presents first the infrared thermography method which is used to visualize the thermal bridges as well as a genuine complementary experimental method allowing for the determination of the quantitative aspects of the heat losses through the envelope. Tangential-gradient heat fluxmeters, which create little disturbance in the measurements, are used in the context of laboratory and in full-scale *in-situ* experiments. Then, the article presents a simple yet accurate prediction with a three-dimensional numerical method that could be used for the design of specific installations and parametric studies.

Keywords: Thermal bridges, infrared thermography, heat fluxmeters, numerical predictions.

Nomenclature

T	Temperature	°C
h	heat transfer coefficient	$W.m^{-2}.K^{-1}$
d	equivalent depth of air cavity	m

[*] Corresponding author : T : +333 2163 7153 ; F : +333 2161 17.80 ; @ : laurent.zalewski@univ-artois.fr ; Faculté des Sciences Appliquées, Technoparc Futura, 62400 BETHUNE, FRANCE

b	equivalent width of air cavity	m

Greek Symbols

ε	emissivity	
λ	Thermal conductivity	$W.m^{-1}.K^{-1}$
θ	Temperature difference	°C
σ	Stefan-Boltzmann constant : 5,67 E^{-8}	$W.m^{-2}.K^{-4}$

Subscripts

i	inside
o	outside
c	convective heat transfer
r	radiative heat transfer
eq	equivalent
ss	steady state
smin	minimum surface temperature
smax	maximum surface temperature
m	mean

1. Introduction

In the past few decades, tremendous developments occurred in the improvements of the thermal efficiency of building envelopes. The political risk of energy shortage in the 1970's [1,2], the perpetual strive for greater indoor comfort, then nowadays the measures to reduce the emission of greenhouse gases, and the spectacular increases in the cost of energy management in buildings, have led to stricter requirements in the different norms and regulations in all European [3] and American countries.

DÉQUÉ et al. [4] in the introduction of their paper, state that "insulating walls represent one of the simplest solutions for decreasing the building's heat losses". However, although quite obvious on the energy balance, the ever improving insulation implies that the relative proportion of the heat losses by the cold bridges in the wall became much more important over the years. Consequently, several studies followed to determine the relative influence of thermal bridges in the overall heat losses. For the calculation of thermal bridges at the interface of the wall sheeting and its structure (caused by the presence of a metal or wooden frame), the method, in the context of standard calculations [5,6,7], consists in integrating (in the evaluation of thermal losses) a linear thermal transmittance (or ψ-value in $W.m^{-1}.K^{-1}$). This method, still used and described in details in the ASHRAE handbook [8], under estimates global heat losses through the walls in most cases [4]. To obtain more realistic results, two-dimensional numerical simulations have been performed [4,9]. In their study, Dilmac et al. [10] compare the results obtained by the methods stated in several standards (ISO 9164, EN832 etc.) with those obtained from 2D analyses in the context of heat loss through floor/beam-wall intersections. It is worth noting that most studies are concerned with linear thermal bridges occurring at the « wall-wall », « wall-ceiling », or « wall-floor » intersections. On the other hand, three-dimensional analyses are sparse so do the unsteady analyses [11,12]. It is this latter phenomenon which is treated herein.

The other major improvement in the study of thermal bridges is this recent possibility for engineers to use performing infrared thermography instruments. This technique allows the visualization of heat losses: 1) *in-situ*; 2) at a distance (without contact); 3) at the scale of the

building; and 4) without intrusion in the building walls (Non-destructive technique). The applications of infrared thermography are not limited to thermal bridges. Balaras and Argiriou [13] suggest it in an exhaustive review of thermal diagnostics for buildings, Wiggenhauser [14] discusses the coupling with moisture analysis in building materials, and the and Bérubé-Dufour et al. [15] focus attention on the use of thermography in the context of crack detection and their evolution in masonry walls. Hence, the IR camera is an efficient tool but requires the understanding of a variety of principles and phenomena, like heat transfers, thermodynamics, optics, fluid physics, electronics, and materials structure [16] for a consequent interpretation of the results (images).

The theme of this paper pertains to experimental measurements on building walls involving thermal bridges caused by steel frame. In such a context, two particular studies were considered as references. First, Haralambopoulos and Paparsenos [17] propose an infrared thermography diagnostic so as to find the zones which are the most thermally representative of the whole building envelope. The overall thermal resistance is then estimated with respect to the heat fluxes and surface temperature measurements The objective is the determination of thermal heat loss levels in order to upgrade the building envelope to modern standards of thermal insulation. Second, Gorgolewski [18], suggests calculation methods for thermal resistance (R-value) and thermal transmittance (U-value) for light steel frame constructions. The building wall investigated is somewhere similar to that used herein. However, the objective is to describe the development of a simplified method for calculating U-values of light steel frame constructions suitable for incorporating into U-value calculation software.

The work proposed here could be very important for the establishment and the improvement of reliable models. In a first step, the proposed methodology involves an infrared camera employed to locate the thermal bridges within a wall involving metal frame, insulating materials, and air gaps. The three modes of heat transfer occur simultaneously within the wall. The IR thermograms are analysed and confronted to local flux and temperature measurements. The first objective is to experimentally quantify surface and linear heat losses. The experimental results are used to validate the numerical predictions obtained with the commercial code commercial TRISCO [19]. This tool allows for steady-state 3D simulations. When the validation

is complete, modifications to the original wall are proposed and parametric studies are carried out to reduce the effect of the thermal bridges.

2. Description of the building wall

The envelope studied here is in conformity with the French regulation (RT2000) with respect to insulation regulations and it does not claim to ensure the appropriate insulation for buildings in the very cold Canadian or Swedish [20] climates, for instance. The wall investigated in this study consists of several building materials embedded in an assembly (Fig.1). The particular feature of this construction process involves assembling a prefabricated steel framework on site (MEPAC process) then adjoining (or inserting) relevant insulation and other materials.

Thermal insulation 10 cm thick is introduced between the vertical frameworks (equally distributed C-shaped steel profiles spaced 60 cm apart, cf. Fig. 1). The mineral wool is protected by a rain barrier on the outside and a vapor barrier on the inside. Both these barriers are held in place by the vertical framework and by horizontal steel with “hat” sections shown in Fig.2. A facing is fixed to these sections. On the outside, this consists of a PREGYBETON panel (cement and polystyrene beads) covered with Polymer Wall Coating, and on the inside of a standard plasterboard panel.

The outside surface of the wall is ventilated by holes drilled into the horizontal steel hat sections (Fig.2). Under high radiative heat fluxes, the PREGYBETON panels heat up and the fluid enters naturally into the external lower part of the wall via a Z-section provided with appropriate apertures and leaves from the upper part through the roof. The aim of this natural ventilation is to avoid the risk of excessive mechanical stress in the outer facing during periods of strong sunlight. The ventilation of this air space should also limit the risks of condensation, which would be harmful for the framework.

On the other hand, the non-perforated hat profiles on the inside of the wall create a partitioned closed air space with a view to increasing the overall thermal resistance of the wall. Interestingly, such a construction should provide good thermal resistance but this particular assembly involves important thermal bridges (Fig. 1). The studies carried out and described

below were intended to demonstrate, quantify, and eventually reduce the heat losses imputable to these bridges.

3. Experimental study

3.1. Experimental set-up

The results presented in this study were obtained from laboratory measurements performed on a wall built between two temperature-regulated climatic cells (Fig. 3). To identify the thermal bridges, the wall was first observed by means of infrared thermography on the "outside" surface. To generate a significant heat flux, a temperature of T_i=42°C was imposed on the "inside" cell whereas the set-point was fixed at approximately T_0=20°C on the "outside". The thermograms recorded were compared with temperature measurements with thermocouples. The second part of the study involved installing tangential-gradient fluxmeters on the standard section of the outer wall and against the vertical framework in order to evaluate the heat fluxes crossing the areas. Heat fluxes can be measured with fluxmeters such as the multi-purpose and yet precise "tangential gradients fluxmeter" designed, built, and improved in our laboratory over the past decade [21,22,23,24]. However, these devices provide local information only and therefore cannot be used to assess the overall heat flux over a surface that may non-uniformly loses energy.

3.2. Infrared thermography

For this study, an Agema 570 PM (8-13,5µm) micro-bolometric array infrared camera was used. It was connected to a laptop computer capable of recording 240x320 pixels thermograms in real time. Recordings were carried out for 24 hours periods with an acquisition time step of 1 minute for a total of 1440 frames per samples. The camera was configured for measurement in an environment at 20°C and 50% of relative humidity. During measurements, the "outside" room temperature varied weakly over a 24h period (between T_0=19°C and T_0=22°C). With respect to heat flux measurements this induces negligible effects of room temperature on the behaviour of the camera [25]. An emissivity of $\varepsilon=0,9\pm0,02$, was measured for the plate of Prégybéton using a BENTHAM spectrometer. The walls which delimit the test cell have emissivities close to

$\varepsilon=0,9\pm0,02$. The measurements of surface emissivities were carefully carried out although the variations of this parameter induce negligible influences upon the surface temperature readings of the camera over the range 0,89 - 0,91. The walls surface temperatures were assumed to be that of still air as the 24 hours period of variations makes the overall system in quasi steady-state. As a cross check, simultaneous measurements of air temperature and resultant temperature measured with a temperature globe confirmed the absence of significant radiative disturbances during the measurements. The camera was located in the doorway of the "outside" cell and was aligned along an axis perpendicular to the wall at a distance of 2.5 m (Fig.3). In Fig.4, T_1 and T_2 are measured with surface thermocouples.

3.3. Preliminary qualitative results

The results presented in Fig.4 clearly illustrate the presence of thermal bridges through the framework. Significant heat loss through the vertical framework is quite obvious (highest temperatures) in the high part of the figure as the vertical yellow lines can clearly be observed. Additional losses are quite less obvious but nevertheless perceptible through the horizontal hat sections. The latter can be explained by the fact that heat is transmitted locally by conduction from the vertical framework to the horizontal hat profiles. It can also be seen that the wall is increasingly hot with height. This corresponds to the normal thermal stratification due to the fact that air is hardly disturbed within the cells despite natural convection. A closer observation indicates that there is no exact symmetry from one section to the next along the x-axis. This is caused by: (1) the irregular surface area of the internal vertical surface (the rain barrier, Fig.2) which depends upon the capacity of the rain barrier to sustain the insulation layer; (2) the asymmetry of the wall on which the test element is inserted in the global x-y plane (Fig.4).

From results presented in Fig. 4, it can be said that it is quite easy to identify thermal bridges using an infrared camera.

However, although these first results make it possible to visualize the problem, they do not allow the quantitative evaluation of the impact of the thermal bridges on the total performances (heat losses) of the wall. They do not allow either concluding as for energy consumption due to the bridges. Indeed, the study becomes more delicate when one wishes to carry out a quantitative analysis [26].

3.4. Surface temperature measurements

To increase the thermal behaviour knowledge of the surface, surface temperature measurements with thermocouples are compared with those provided by the infrared camera. Fig.5 shows the evolution of the outside temperature, T_o, over a period of about 20 hours. In this figure, the temperature variations (sudden drop, asymptotic increase) are due to the cyclic variations of the building environment itself. It was not possible to heat the “outside” cell to maintain a constant temperature as the source would have induced perturbations in the camera readings. The natural temperature variations are indeed preferable as they introduce, as mentioned earlier, a negligible bias in the readings. The thermocouples were calibrated in a temperature calibrator (CS172 Eurolec). Nevertheless, there is a maximum difference of 0,5°C between the two thermocouples located symmetrically compared to the vertical framework (Fig.4-5). This variation falls within the measurement uncertainties on the surface temperature measurement but can also be explained by actual differences that can exist between apparently symmetric zones of the wall (compression of insulator, variable thickness of the air layer, etc., Fig.2). In Fig.5, a maximum of one degree difference is shown between the thermocouple readings for surface temperature and the value, provided after image processing, recorded by the infrared camera. This relatively low difference can be explained by: (1) uncertainty on the calibration of the camera itself; (2) the uncertainty on the surface’s emissivity (±0.02) [27]; (3) the uncertainty on thermocouple temperature measurements (±0,5 °C), (4) the uncertainty on ambient hygroscopy (50%±5%); (5) the variation of 19°C to 22°C of the ambient temperature; (6) the background radiation emitted by the environment directly on to the camera lens [28]; or (7) by the reflection of the radiative heat flux on (by) the wall. Determination of the surface temperatures in various areas of the surface shows that thermal bridges do exist but it does not enable to provide an estimate of the heat flux.

3.5. Heat flux measurements

To overcome the aforementioned problem, the use of heat flux sensors is suggested in the following experiment. The sensors used are of “tangential gradient type” [29,30]. The tangential gradient fluxmeter intrinsically generates temperature variations in the plane of measurements. Then, these gradients are detected by a great number of thermoelectric junctions connected in

series. Indeed, the sensor generates a Seebeck electro motive force (EMF) which is proportional to the heat flux. These fluxmeters have a highly conductive copper surface which tends to homogenize the surface temperature and thus to provide average values. The fluxmeters are calibrated by use of the null flux method [31]. Three fluxmeters with a sensitive area of 15x15 cm² and a response time of about 1 second were used for this experiment: two of them were located (Fig.6) on the standard sections, q_1 and q_3, while the third, the middle one q_2, was located above a vertical steel frame. The average calibration for each fluxmeter is 100 $\mu V/W.m^2$. In order to avoid heat losses from the edges of the sensors or in other words to ensure that the heat flow is unidirectional in the zone of measurement, a guard zone was systematically installed around each sensor. (A guard zone is a non-active part of the surface of a sensor having the same thermophysical properties as the active zone). In this configuration, each sensor measures the local average heat flux in the z-direction, over its surface, between the wall and its environment (Fig. 6).

In order to show the importance of the thermal bridges and their evolution in dynamic transfer, an unsteady temperature difference was imposed between the two faces of the wall. The results for the three fluxmeters over a 48 hours period are presented Fig.7. This figure indicates that heat losses from the second fluxmeter, (q_2), located above the steel structure, are twice as important as those for the standard section (q_1 and q_3). The very small thermal inertia of such walls makes the surface temperatures change very quickly according to the changes of the ambient room temperature. Similar conclusions hold for heat fluxes. Moreover, although theses fluxes are very low (as the wall is well insulated), Fig.7 indicates that the heat fluxes are measurable. Taking into account the overall uncertainties during the calibration (5%) [31], this simple experimentation demonstrates that the thermal heat losses caused by the thermal bridges can be evaluated. It also confirms what was observed visually by infrared thermography.

However, this experiment is a first approach. Indeed, the measured heat fluxes are available only for limited locations (three in this experiment) and are function of the sensors dimensions. In order to evaluate how far these thermal bridges increase overall heat losses from the wall, a larger number of fluxmeters would be required, covering a representative area

of the average characteristics of the wall. Another way to evaluate the effect of these thermal bridges is to model the entire wall and to benchmark critical locations with appropriate local heat flow measurements. This approach will enable the global predictions of the heat losses on a complete wall. This approach is presented in the next section.

4. Numerical study

4.1. Global issues

The objective is to propose a suitable numerical prediction tool that will enable the analyst to first identify the worst areas of heat lost and, consequently, to perform design corrections to reduce these losses. Hence, the MEPAC experimental building envelope was modelled with commercial thermal analysis software called "TRISCO" [29]. The version employed is restricted to steady-state three-dimensional conductive heat transfer but enables ~~one~~ to treat complex geometries. However, it is restricted to the use of Cartesian structured grids based upon parallelepiped components. The software requires appropriate domain discretization and proper boundary conditions prescription. Then, a system of linear equations based on the energy balance technique [18] is solved by use of an efficient iterative method.

4.2. Domain discretization

The domain discretization is quite straightforward as the vapour and water barriers resistances are neglected and no contact resistances are considered as the insulation layer provides, and by far, the strongest resistance. The only twist in the domain discretization is that TRISCO does not take into account non-rectangular elements. Hence, this led us to represent the hat sections (Fig, 2) by assemblies of rectangular elements with the same surface areas of contact in order to reproduce, as accurately as possible, the real heat transfers. Fig. 9 schematically describes the transformation. The air gaps are modelled with equivalent thermal conductivities evaluated according to specific values taken from a database embedded within the software (See section 4.4). The problem can then be thought of as a simple three-dimensional conductive heat transfer problem. The surface area of the investigated wall is 5.39 m², which corresponds to four vertical

bays and one floor in height (2.50m). Fig. 8 shows the typical domain discretization used involving 245712 nodes which was found to be sufficient to provide convergence and no difference in the solutions with further refinement.

4.3. Boundary conditions

Boundary conditions are prescribed as surface temperatures on the outside and inside boundaries and an adiabatic condition is imposed at the wall periphery. The experimental ambient temperatures (Ti = 42°C and To = 21°C) were chosen to match the actual measurements carried out at instant t=5h00 (Fig.7). These results were used as the wall for this period was found to be in nearly steady-state and because of the limitation embedded within the used version of TRISCO.

4.4. Modeling of air spaces

As the overall temperature difference imposed in this experiment is low (about 20^{o}C), without intensive sun solicitations, it was found in a previous study [32] that the air flow in the ventilated layer (Fig.2) of the wall is negligible. The experimental study conducted on the air layer, its geometric dimensions (narrowness) and the presence of small holes in the hat sections (generating high pressure losses) led to the assumption in this model that this outside air layer is not actually ventilated. As the openings cross-sections in these hat sections are very small in relation to their overall cross-sections, they create only small areas where convective movement has much difficulty to develop. Consequently, a vertical series of cavities separated by horizontal steel elements is obtained (Fig. 10). The layer indeed allows air flow only when direct solar heat flux occurs which is not the case in the present laboratory experiment. Hence, automatic calculations of an equivalent thermal conductivity for the air cavities on both sides are modelled as materials. The "RADCON" [33] module is used to link radiation and convection within the air gaps to the equivalent thermal conductivity.

4.5. Equivalent thermal conductivity

To model the heat transfers in a non-ventilated space, the principle is to use the concept of equivalent conductivity. TRISCO allows calculating the equivalent thermal conductivity of air

cavities according to EN ISO 6946. The equivalent thermal conductivity λ_{eq} [W/(m.K)] is calculated using the following formula: $(h_c+h_r).d$. In which : h_c = convective heat transfer coefficient [W/(m^2.K)], h_r = radiative heat transfer coefficient [W/(m2.K)] and d = equivalent depth of the air cavity [m] (parallel to the heat flow direction).

The convective heat transfer coefficient (surface to surface) h_c [W/(m2.K)] is calculated as follows :

$$h_c = \max\left\{\frac{C_1}{d},\quad \frac{C_2\cdot\left(\Delta\theta_{ss}\cdot d^3\right)^{C_3}}{d}\right\} \tag{1}$$

with: d = equivalent depth [m], $\Delta\theta_{ss}$ = maximum surface temperature difference in the air cavity [°C]

The maximum surface temperature difference $\Delta\theta_{ss}$ is taken constant when no solution results are available (For EN ISO 6946: use 5°C). The parameters C_1, C_2 and C_3 , for an horizontal heat flow, are C_1 = 0.025, C_2 = 0.73 and C_3 = 0.333333.

The radiative heat transfer coefficient h_r [W/(m^2.K)] is calculated as follows :

$$h_r = \frac{1}{\frac{1}{\varepsilon_1}+\frac{1}{\varepsilon_2}-1}\cdot 2\sigma\cdot\left(\theta_m+273.16\right)^3\cdot\left(1+\sqrt{1+\left(\frac{d}{b}\right)^2}-\frac{d}{b}\right) \tag{2}$$

with: ε_1, ε_2 = emissivity at both sides of the air cavity (in the direction of the heat flow), σ = 5,67 10^{-8} W/m^2K^4 (Stefan-Boltzmann constant), θ_m = mean temperature in the air cavity [°C], b : equivalent width of the air cavity [m]. The emissivities ε_1 and ε_2 are estimated to be about 0,9 for the materials and 0,1for the galvanized steel. This assumption is mostly appropriate as modifications of radiative transfers predictions were observed only for emissivity variations exceeding 10%. The mean temperature θ_m is automatically calculated as:

$\theta_m = \left(\theta_{smin}+\theta_{smax}\right)/2$ with: θ_{smin} : minimum surface temperature in air cavity [°C], θ_{smax} = maximum surface temperature in air cavity [°C].

4.6. Validation of the model

Fig. 11 presents results for the temperature field throughout the calculation domain subject to the prescribed boundary conditions. A section of the external face of the wall is shown in blue. These qualitative results for the temperature field clearly confirm the presence of thermal bridges in the MEPAC shell. As on the thermogram presented in Fig. 4, the thermal bridges remain mostly obvious at the level of the vertical framework.

4.7. Heat flux predictions

The representation of heat flux across the wall is presented in Fig. 12. This figure indicates that heat losses through the vertical framework are twice as important as those in the standard section. A comparison between the fluxmeter measurements and these numerical predictions validates the assumptions embedded within the model (boundary conditions, thermophysical properties of the materials, calculation assumptions, discretization technique, etc.). The heat fluxes measured and calculated in the standard section are both about 4.0 W/m² while those for the area located above the vertical framework provide an average value of 9 W/m² for the measurements over the area of the fluxmeter, q_2, and a variation from 7 W/m² to 11.5 W/m² for the predictions. These results as well as those for temperature predictions provide excellent confidence in the propose mode to perform numerical analyses of the MEPAC wall assembly.

4.8. Heat flux reduction

With a suitable model, it is possible to evaluate the relative influence of the thermal bridges on overall heat losses from the wall. This is done here by first eliminating the vertical steel framework from the model. Predictions indicate that the overall heat transfer coefficient per unit area of the wall is 0.320 $W.m^{-2}.°C^{-1}$ for the actual construction and that it would be 0.236 $W.m^{-2}.°C^{-1}$ for the same wall without any steel framework. The thermal bridges thus increase overall heat losses from the wall by 26.2% (cf. table1).

From the construction point of view, it is not possible to completely eliminate the vertical framework as this represents the trademark and design characteristic of MEPAC. A technical solution would nevertheless involve breaking the thermal bridge inside the wall. One way, suggested and tested here, consists in replacing the unventilated air space on the inside by an

insulating assembly. Adding 4 cm of insulating material along with a 1 cm thick plasterboard inside would make the overall heat transfer coefficient per unit area of wall (Ug) equal to 0.235 $W.m^{-2}.°C^{-1}$. If the steel frame is not taken into account, the coefficient is in this case is 0.194 $W.m^{-2}.°C^{-1}$. Replacing the air layer with the insulating complex would reduce overall heat losses from the wall by about 27% (26.7% : cf. cf. table1) and reduce the relative importance of the thermal bridges to 17.3%.

In another simulation, the same calculation is carried out with an increased insulating thickness (8cm + 1cm plasterboard). This would lead to a reduction of 41.8% in heat losses in relation to the reference wall and would reduce the share of the thermal bridges to 13.5%.

5. Conclusion

In this study, an original method allowing measurements of the quantitative influence of thermal bridges resulting from the presence of a steel frame in the envelope of buildings was proposed. The relative importance of thermal bridges increases in the energy balance of recent highly insulated buildings. It requires a very detailed attention with the components of the envelope and their implementation. Moreover, to ensure an extended life cycle for the buildings, it is vital to reduce these singularities as well as possible in order to avoid any problem of internal condensation which would be prejudicial to the framework and to the performances insulating materials. An infrared camera made it possible to visualize and thus to precisely locate the zones of influence of the steel frame on the thermal bridges. But this method answers only part of the problem by converting surface variations of temperature into nuances of colour on a thermogram. Furthermore, with no quantitative evaluation of heat fluxes, the thermogram can only be used with care because many parameters may disturb readings (variations of surfaces emissivity, room temperature, relative moisture, parasitic infra-red radiations, solar radiations, etc.).

This work demonstrated that heat flux measurements can be carried out locally and easily by used of appropriate fluxmeters. A light wall with steel frame was instrumented, measurements show that the heat losses in front of the steel frame are twice much important as elsewhere. The local and non-destructive flux measurements were also proven to be very useful to establish

and validate simulation model. The paper briefly indicated how this double approach of experimentation and numerical modelling makes it possible to validate certain assumptions concerning the thermal performance of the wall then to optimize it to reach the best possible performances.

The results obtained in laboratory and *in-situ*, lead to discussions with the designer using the MEPAC assembly. The study made it possible to consider several choices for wall composition in full safety. Modifications suggested compared to the initial wall appeared very relevant, for example by replacing a non-ventilated air layer by a rigid insulation. Comparisons between steel frame and wood frame (not discussed here) also showed all the interest of these measurements combined with the numerical thermal optimization of the buildings envelopes.

Acknowledgments

The authors would like to thank the office H.L.M. "PAS-DE-CALAIS HABITAT" which is at the origin of this study and which partly financed the thesis work of Mr. BOUKHALFA; EDF and GDF which financed the rest of the thesis and for their implication in the study. We also make a point of thanking the Region NORD-PAS-DE-CALAIS through the "ACTION DE RECHERCHE CONCERTEE INGENIERIE URBAINE" and the European Community (FEDER) which by their financial support allowed the acquisition of equipment and measuring instruments used in this work. The fourth author is also grateful to the Natural Sciences and Engineering Research Council of Canada (NSERC) for a discovery grant.

Figure and table captions

Fig. 1: Cross-section of shell

Fig. 2: Vertical section (side view)

Fig. 3: Shell separating the experimental cells

Fig. 4: Typical thermogram

Fig. 5: Comparison of temperature evolution: thermocouples vs infrared thermography

Fig. 6: Locations of tangential gradients fluxmeters

Fig. 7: Unsteady heat fluxes measurements on the outside wall over a 48 hours period

Figures

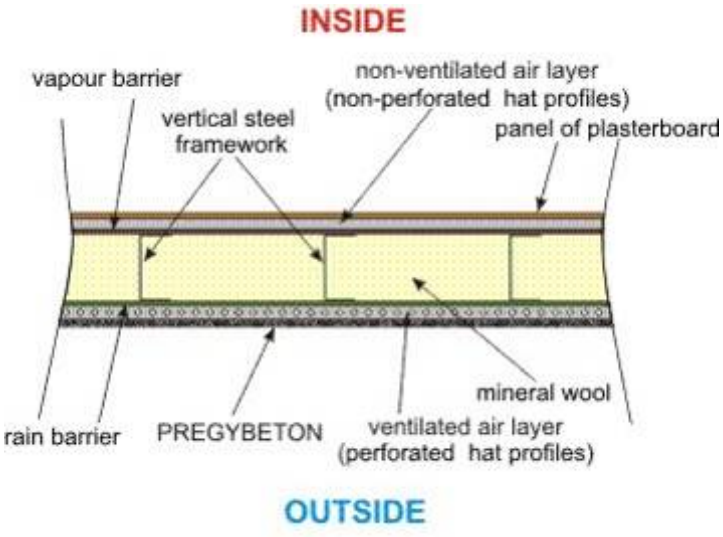

Fig. 1: Cross-section of shell (plane view)

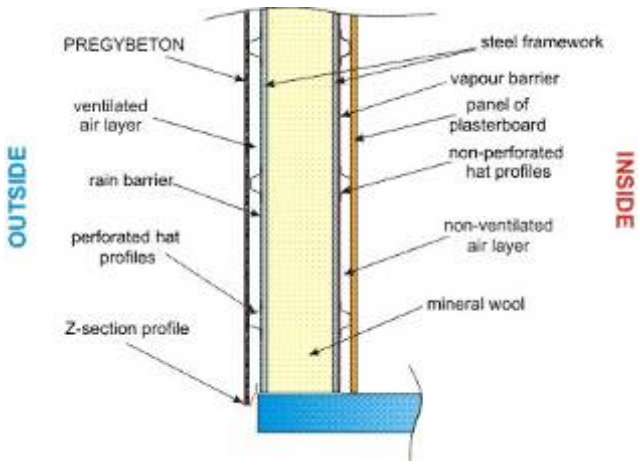

Fig. 2: Vertical section (side view)

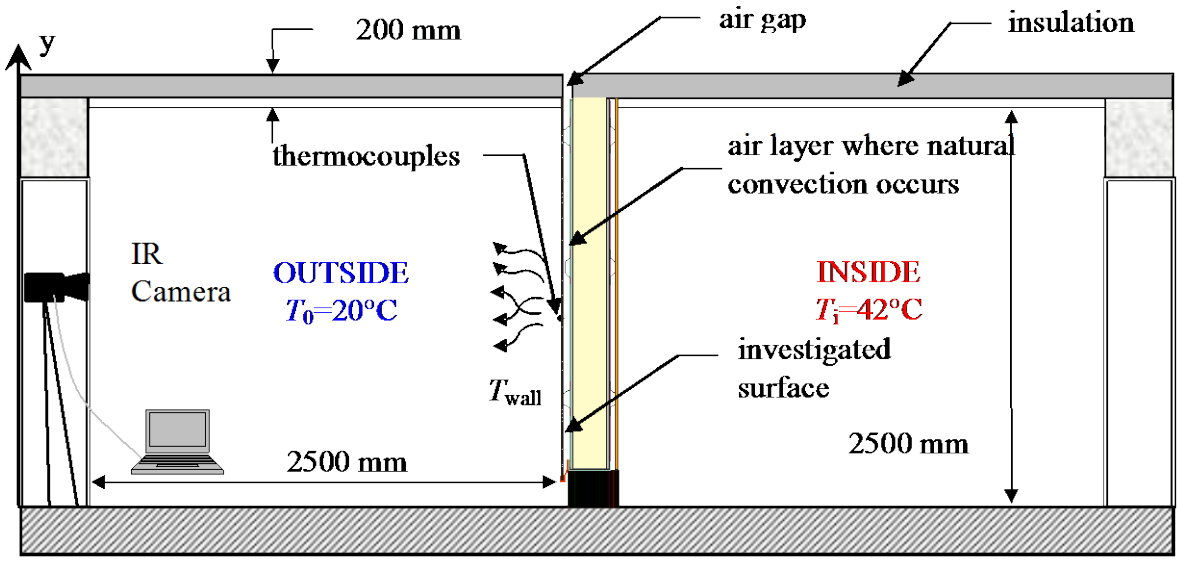

Fig. 3: The overall experimental set-up

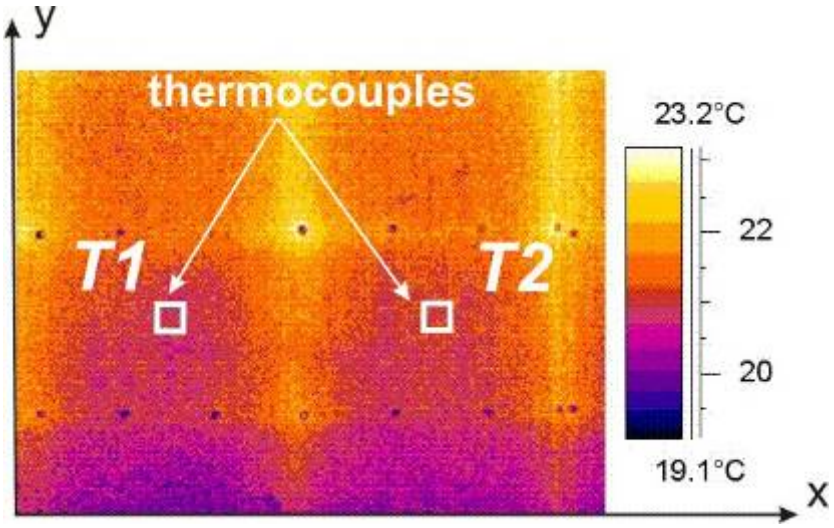

Figure 4: Thermogram of the “outside” surface

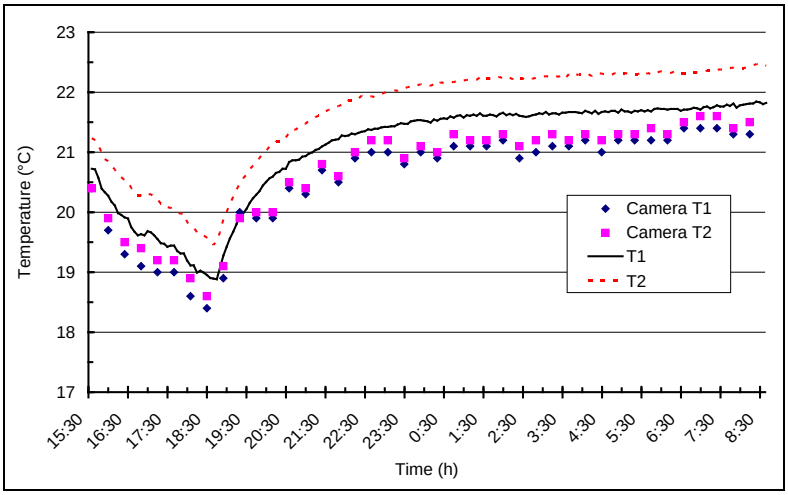

Fig. 5: Comparison of temperature evolution: thermocouples vs infrared thermography

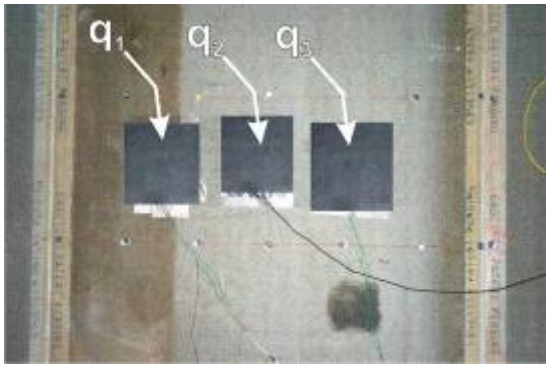

Fig. 6: Locations of tangential gradients fluxmeters

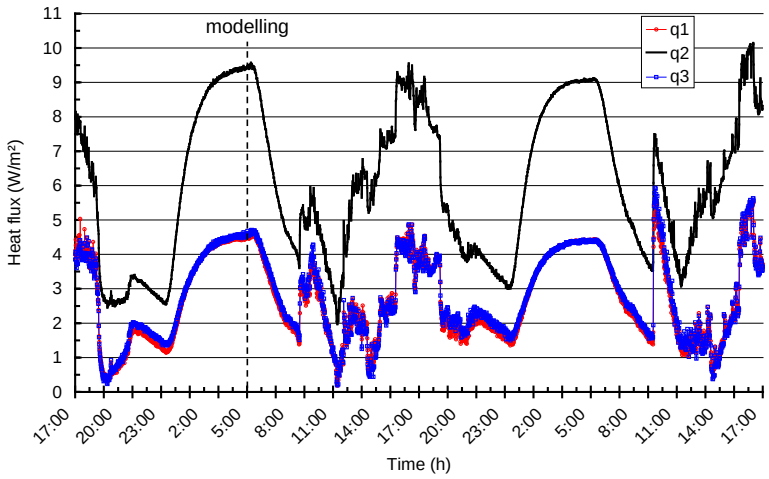

Fig. 7: Unsteady heat fluxes measurements on the outside wall over a 48 hours period

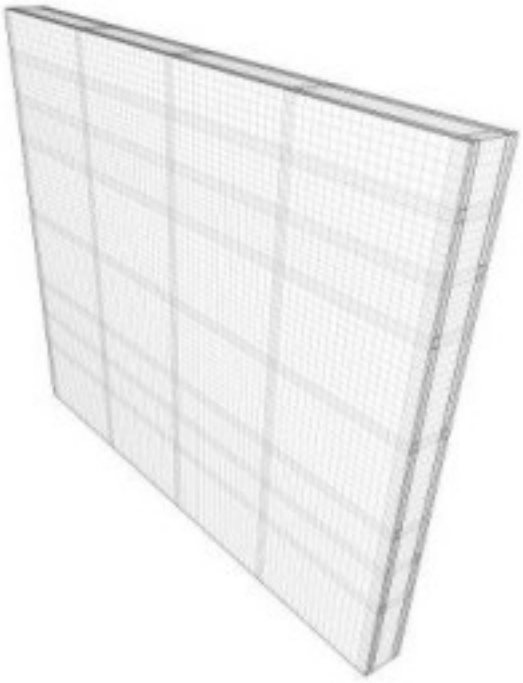

Fig. 8: The domain structured-grid Cartesian discretization involving 245712 nodes.

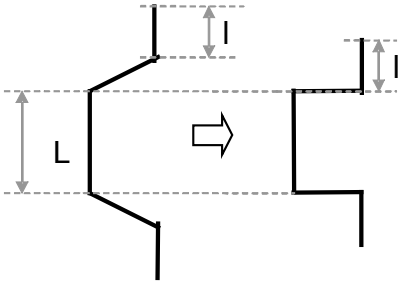

Fig. 9: Geometry transformation adopted for the “hat” sections.

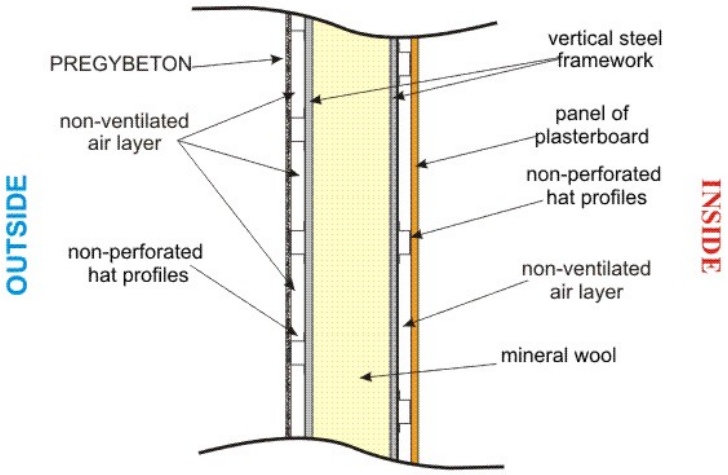

Fig. 10: Actual calculation domain after geometric modifications.

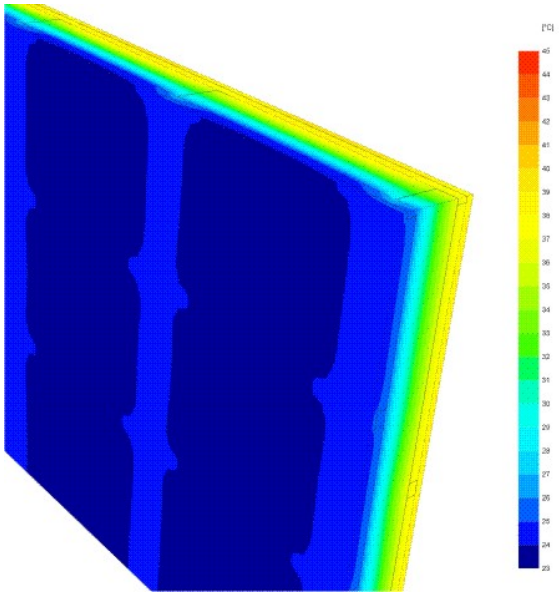

Fig. 11: Predictions of the temperature field

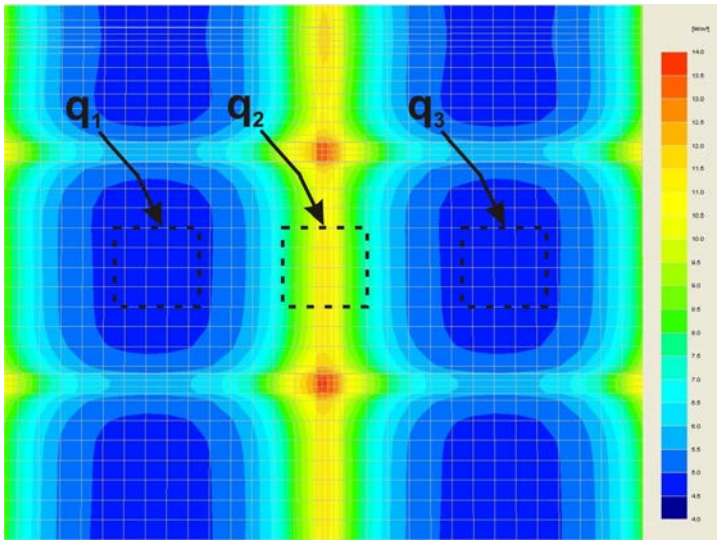

Fig. 12: Heat flux predictions across the wall : q_1 and q_3 located above standard sections ; q_2 located above a section involving a steel frame.

Tables

	U global ($W.m^{-2}.°C^{-1}$)	U no thermal bridges ($W.m^{-2}.°C^{-1}$)	Relative importance of the thermal bridges (%)
Inside air layer	**0,32**	**0,236**	**26,2%**
Insulating complex (4+1cm)	**0,235**	**0,194**	**17,3%**
Insulating complex (8+1cm)	**0,186**	**0,161**	**13,5%**

-26,7%

-41,8%

Table 1: Overall heat transfer coefficient predictions for selected insulating strategies with and without steel frame.

[1] E. Hirsta, D. O'Neal, Contributions of improved technologies to reduced residential energy growth, Energy and Buildings, Vol. 2, Issue 3, (1979) pp. 217-224
[2] E. Hirst, R. W Barnes., S. M. Cohn, K. R. Corum, D. Greene, D. M. Hamblin, G. Kulp, D. B. Reister and T. Vineyard A., Effects of improved energy efficiency on U.S. energy use: 1973–1980, Energy, Vol. 7, Issue 11, (1982), pp897-907
[3] Communication from the commission, Action Plan for Energy Efficiency: Realising the Potential, Brussels, 19.10.2006, (http://ec.europa.eu/energy/action_plan_energy_efficiency/doc/com_2006_0545_en.pdf)
[4] F. Déqué, F. Ollivier, J. J. Roux, Effect of 2D modelling of thermal bridges on the energy performance of buildings: Numerical application on the Matisse apartment, Energy and Buildings, Vol. 33, Issue 6, (2001), pp583-587
[5] Ministère de l'équipement, Guide de la réglementation thermique, France, (2000)
[6] EN ISO 14683, Thermal bridges in building construction: linear thermal transmittance, Simplified methods and default values, (2000)

[7] Thermal bridges in building construction. Heat flows and surface temperatures. Detailed calculations, EN 10211, ISBN : 978 0 580 64346 0
[8] ASHRAE Handbook—Fundamentals, (2005) , CHAPTER 25 : Thermal and water vapor transmission data
[9] A.Ben Larbi, Statistical modelling of heat transfer for thermal bridges of buildings, Energy and Buildings, Vol. 37, Issue 9, (2005) , pp945-951
[10] S. Dilmac, A. Guner, F. Senkal, S. Kartal, Simple method for calculation of heat loss through floor/beam-wall intersections according to ISO 9164, Energy Conversion and Management, Vol. 48, Issue 3, (2007) , pp826-835
[11] M. Guofeng, J. Gudni, Dynamic calculation of thermal bridges, Energy and Buildings, Vol. 26, Issue 3, (1997) , pp233-240
[12] Jan Kosny, Elizabeth Kossecka,Multi-dimensional heat transfer through complex building envelope assemblies in hourly energy simulation programs, Energy and Buildings, Vol. 34, Issue 5, (2002) , pp445-454
[13] C. A. Balaras, A. A. Argiriou, Infrared thermography for building diagnostics, Energy and Buildings, Vol. 34, Issue 2, (2002) , Pages 171-183
[14] H. Wiggenhauser, Active IR-applications in civil engineering, Infrared Physics & Technology, Vol. 43, Issues 3-5, (2002) , pp233-238
[15] M. Bérubé Dufour, D. Derome, R. Zmeureanu, Analysis of thermograms for the estimation of dimensions of cracks in building envelope, Infrared Physics & Technology, Vol. 52, Issues 2-3, (2009) , pp70-78
[16] S. Ribarić, D. Marčetić, D. Stjepan Vedrina, A knowledge-based system for the non-destructive diagnostics of façade isolation using the information fusion of visual and IR images, Expert Systems with Applications, Vol.36, Issue 2, Part 2, (2009) , pp 3812-3823
[17] D. A. Haralambopoulos, G. F. Paparsenos, Assessing the thermal insulation of old buildings—The need for in situ spot measurements of thermal resistance and planar infrared thermography, Energy Conversion and Management, Vol.39, Issues 1-2, (1998), pp65-79
[18] M. Gorgolewski, Developing a simplified method of calculating U-values in light steel framing., Int. Rev. Building and Environment, Vol.42, (2007), pp 230-236
[19] P.Standaert, Computer program to calculate 3D & 2D steady state heat transfer in objects described in a rectangular grid using the energy balance technique, Physibel document TRISCO V10.0 w Manual, (2002)
[20] T. Höglund, H. Burstrand, Slotted steel studs to reduce thermal bridges in insulated walls, Thin-walled Structures 32, (1998), pp81-109
[21] O. Carpentier, D. Defer, E. Antczak, A. Chauchois, B. Duthoit, In situ thermal properties characterization using frequential methods, Energy And Buildings, Vol.40, Issue 3, (2008), pp300-307
[22] E.Antczak, A. Chauchois, D.Defer, B. Duthoit, Characterisation of the thermal effusivity of a partially saturated soil by the inverse method in the frequency domain, Applied Thermal Engineering, 2003, vol. 23, issue 12, p.1525-1536
[23] D. Defer, E. Antczak, B. Duthoit, Measurement of low thermal effusivity of building materials using thermal method account, Measurement Sciences and Technologie, 2001, Vol 12, p 1-8
[24] L. Zalewski, S. Lassue, B Duthoit, Butez M., Study of solar wall - validating a simulation model, Building and Environnement, Vol.37, (2002) , pp109-121
[25] AGEMA 570 - Operating Manual,
[26] E. Grinzato, V. Vavilov, T. Kauppinen, Quantitative infrared thermography in building, Energy and building, vol.29, Issue1, (1998), pp1-9.
[27] N.P. Avdelidis, A. Moropoulou, Emissivity considerations in building thermography, Energy and building, vol.35, (2003), Issue 7, pp663-667.
[28] M.R. Clark. D.M. Mc Cam, M.C. Forde, Application of infrared thermography to the non destructive testing of concrete and masonry bridges, NDT & E International, Vol.36, Issue 4, (2003) , pp265-275.
[29] D. Leclercq, P. Thery, Apparatus for simultaneous temperature and heat flow measurement under transient conditions, Rev. of Scient Instrum., Vol.54, (1983) , pp374-380
[30] P. Thureau, Fluxmètres thermiques, Technique de l'ingénieur, 1996
[31] D.L. Marinoski, S. Guths, F.O.R. Pereira, R. Lamberts, Improvement of a measurement system for solar heat gain through fenestrations, Energy and Buildings 39 (2007) 478–487.

[32] K. Boukhalfa, L. Zalewski, S. Lassue, Étude des transferts thermiques au sein d'une lame d'air faiblement ventilée. VIIème Colloque Interuniversitaire Franco-Québécois sur la Thermique des Systèmes. (2005) , Saint-Malo-FRANCE. CIFQ2005 / ART-01-14.
[33] Physibel software, http://www.physibel.be/